Coupled Transmission Line Networks in an Inhomogeneous Dielectric Medium

GEORGE I. ZYSMAN, MEMBER, IEEE, AND A. KENT JOHNSON, MEMBER, IEEE

Abstract—**In this paper, two-port networks composed of two identical, coupled transmission lines embedded in an inhomogeneous dielectric (e.g., suspended substrate, microstrip) are investigated. The *ABCD* parameters of circuit configurations, considered by Jones and Bolljahn [1], are obtained for the case of inhomogeneous dielectric. Equivalent circuits of these networks are also given. It is shown that the characteristics of such circuits differ markedly from those embedded in a homogeneous medium. In addition, experimental results are presented for three types of circuits which have been constructed and tested. There is excellent agreement between the experimental results and those predicted theoretically on the basis of the equivalent circuits.**

I. Introduction

THE PURPOSE of this paper is to examine the nature of the electromagnetic coupling which exists between parallel conductors in an inhomogeneous dielectric such as the suspended substrate. In particular, we consider the network structures that are obtained from two identical coupled lines by placing open or short circuits on various terminal pairs or connecting together two terminals. These circuits were investigated by Jones and Bolljahn [1], in a homogeneous dielectric environment. It is found that the characteristics of coupled-line circuits in a suspended substrate configuration may differ markedly from those in a homogeneous medium. This difference in behavior is due to the fact that the even and odd mode signals, which are commonly used in the analysis of such coupled lines, propagate with unequal phase velocities. This difference in phase velocities precludes a pure TEM wave propagation. It is known, however, that the TEM approximation yields excellent results to several gigahertz and it will be used throughout this analysis.

In order to derive the parameters of the two-port circuits, one considers first the current and voltage relationships which exist on a pair of infinitely long transmission lines. These equations are available in the literature, e.g., Rice [2], Vlostovskiy [3], and Murray [4]. The current–voltage relationships may be cast in the form of impedance, admittance, and chain matrices. The descriptions of the various circuit configurations are then derived by an application of the appropriate boundary conditions. For quantitative results the even and odd mode propagation constants and characteristic impedances must be obtained numerically first. This can be done by a method developed by Smith [5] whose results are used here.

Manuscript received January 29, 1969; revised April 25, 1969. This work was supported by the U. S. Army under Contract DA-30-069-AMC-333(Y).

The authors are with Bell Telephone Laboratories, Inc., Whippany, N. J. 07981.

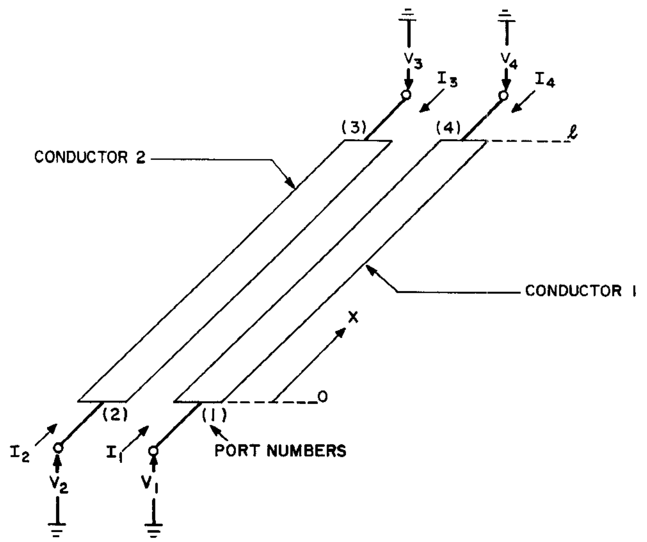

Fig. 1. Schematic of pair of coupled-lines.

II. Coupled-Line Chain, Impedance, and Admittance Matrices

The system of two parallel coupled lines is shown in Fig. 1. In order to obtain the terminal behavior of such a network, the voltages and currents at a point $x=l$ must be related to the voltages and currents at $x=0$. In order to derive the four-port chain matrix for lossless lines, symmetric and antisymmetric excitations of the ports are considered. In the symmetric (even mode) case,

$$\begin{bmatrix} \frac{1}{2}(V_1+V_2) \\ \frac{1}{2}(I_1+I_2) \end{bmatrix} = \begin{bmatrix} \cos\theta_e & jZ_{0e}\sin\theta_e \\ jY_{0e}\sin\theta_e & \cos\theta_e \end{bmatrix} \cdot \begin{bmatrix} \frac{1}{2}(V_4+V_3) \\ -\frac{1}{2}(I_4+I_3) \end{bmatrix}, \tag{1}$$

in the antisymmetric (odd mode) case,

$$\begin{bmatrix} \frac{1}{2}(V_1-V_2) \\ \frac{1}{2}(I_1-I_2) \end{bmatrix} = \begin{bmatrix} \cos\theta_o & jZ_{0o}\sin\theta_o \\ jY_{0o}\sin\theta_o & \cos\theta_o \end{bmatrix} \cdot \begin{bmatrix} \frac{1}{2}(V_4-V_3) \\ -\frac{1}{2}(I_4-I_3) \end{bmatrix}, \tag{2}$$

where

$Y_{0e} = \dfrac{1}{Z_{0e}}$ is the even mode characteristic admittance,

$Y_{0o} = \dfrac{1}{Z_{0o}}$ is the odd mode characteristic admittance,

$\theta_e = \beta_e l = \dfrac{\pi}{2}\,\dfrac{f}{f_{0e}}$ is the even mode electrical length of the lines,

$\theta_o = \beta_o l = \dfrac{\pi}{2}\,\dfrac{f}{f_{0o}}$ is the odd mode electrical length of the lines.

In these equations f_{0e} is the frequency at which the coupled lines are a quarter-wavelength long electrically when excited in the even mode, and f_{0o} is the corresponding frequency for the coupled lines excited in the odd mode.

From (1) and (2) one can derive four simultaneous equations in the port parameters and obtain the four-port chain matrix:

$$\begin{bmatrix} V_1 \\ V_2 \\ I_1 \\ I_2 \end{bmatrix} = \left[\begin{array}{cc|cc} a_{11} & a_{12} & b_{11} & b_{12} \\ a_{21} & a_{22} & b_{21} & b_{22} \\ \hline c_{11} & c_{12} & d_{11} & d_{12} \\ c_{21} & c_{22} & d_{21} & d_{22} \end{array}\right] \begin{bmatrix} V_4 \\ V_3 \\ -I_4 \\ -I_3 \end{bmatrix} \tag{3a}$$

where

$$a_{11} = a_{22} = d_{11} = d_{22} = \tfrac{1}{2}(\cos\theta_e + \cos\theta_o), \tag{3b}$$
$$a_{12} = a_{21} = d_{12} = d_{21} = \tfrac{1}{2}(\cos\theta_e - \cos\theta_o), \tag{3c}$$
$$b_{11} = b_{22} = j\tfrac{1}{2}(Z_{0e}\sin\theta_e + Z_{0o}\sin\theta_o), \tag{3d}$$
$$b_{12} = b_{21} = j\tfrac{1}{2}(Z_{0e}\sin\theta_e - Z_{0o}\sin\theta_o), \tag{3e}$$
$$c_{11} = c_{22} = j\tfrac{1}{2}(Y_{0e}\sin\theta_e + Y_{0o}\sin\theta_o), \tag{3f}$$
$$c_{12} = c_{21} = j\tfrac{1}{2}(Y_{0e}\sin\theta_e - Y_{0o}\sin\theta_o). \tag{3g}$$

The impedance and admittance parameters are derived in a similar fashion. These are:

$$\begin{aligned} Z_{11} &= Z_{22} = Z_{33} = Z_{44} \\ &= -j\tfrac{1}{2}[Z_{0e}\cot\theta_e + Z_{0o}\cot\theta_o], \end{aligned} \tag{4a}$$
$$\begin{aligned} Z_{12} &= Z_{21} = Z_{34} = Z_{43} \\ &= -j\tfrac{1}{2}[Z_{0e}\cot\theta_e - Z_{0o}\cot\theta_o], \end{aligned} \tag{4b}$$
$$\begin{aligned} Z_{13} &= Z_{31} = Z_{24} = Z_{42} \\ &= -j\tfrac{1}{2}[Z_{0e}\csc\theta_e - Z_{0o}\csc\theta_o], \end{aligned} \tag{4c}$$
$$\begin{aligned} Z_{14} &= Z_{41} = Z_{23} = Z_{32} \\ &= -j\tfrac{1}{2}[Z_{0e}\csc\theta_e + Z_{0o}\csc\theta_o], \end{aligned} \tag{4d}$$

and

$$\begin{aligned} Y_{11} &= Y_{22} = Y_{33} = Y_{44} \\ &= -j\tfrac{1}{2}[Y_{0e}\cot\theta_e + Y_{0o}\cot\theta_o], \end{aligned} \tag{5a}$$
$$\begin{aligned} Y_{12} &= Y_{21} = Y_{34} = Y_{43} \\ &= -j\tfrac{1}{2}[Y_{0e}\cot\theta_e - Y_{0o}\cot\theta_o], \end{aligned} \tag{5b}$$
$$\begin{aligned} Y_{13} &= Y_{31} = Y_{24} = Y_{42} \\ &= +j\tfrac{1}{2}[Y_{0e}\csc\theta_e - Y_{0o}\csc\theta_o], \end{aligned} \tag{5c}$$
$$\begin{aligned} Y_{14} &= Y_{41} = Y_{23} = Y_{32} \\ &= +j\tfrac{1}{2}[Y_{0e}\csc\theta_e + Y_{0o}\csc\theta_o]. \end{aligned} \tag{5d}$$

The impedance parameters agree with those derived by Jones and Bolljahn [1] for the case of equal phase velocities. The admittance parameters Y_{12} and Y_{14} do not agree. The admittance values given here have been rechecked by obtaining the product of the impedance and admittance matrices and comparing it with the unit matrix.

III. Symmetric Interdigital Circuits

With the above parameters available it is now possible to derive Y and Z matrices and equivalent circuits for the two fundamental networks of an interdigital filter. These are obtained by either short-circuiting or open-circuiting ports 2 and 4 of Fig. 1. The open-circuited case will be considered first. Opening these two ports imposes the boundary condition

$$I_2 = I_4 = 0.$$

The remaining two-port is then described by the following matrix equation:

$$\begin{bmatrix} V_1 \\ V_3 \end{bmatrix} = \begin{bmatrix} Z_{11} & Z_{13} \\ Z_{31} & Z_{33} \end{bmatrix} \begin{bmatrix} I_1 \\ I_3 \end{bmatrix} \tag{6}$$

where

$$\begin{aligned} \begin{bmatrix} Z_{11} & Z_{13} \\ Z_{31} & Z_{33} \end{bmatrix} &= -j\frac{1}{2}\left[\begin{array}{c|c} Z_{0e}\cot\theta_e + Z_{0o}\cot\theta_o & Z_{0e}\csc\theta_e - Z_{0o}\csc\theta_o \\ Z_{0e}\csc\theta_e - Z_{0o}\csc\theta_o & Z_{0e}\cot\theta_e + Z_{0o}\cot\theta_o \end{array}\right] \\ &= -j\frac{Z_{0e}}{2}\left[\begin{array}{c|c} \cot\theta_e & \csc\theta_e \\ \hline \csc\theta_e & \cot\theta_e \end{array}\right] - j\frac{Z_{0o}}{2}\left[\begin{array}{c|c} \cot\theta_o & -\csc\theta_o \\ \hline -\csc\theta_o & \cot\theta_o \end{array}\right]. \end{aligned} \tag{7}$$

Now the Z matrix for a simple unit element (i.e., length of line of electrical length θ) is

$$[Z] = -jZ_0\begin{bmatrix} \cot\theta & \csc\theta \\ \csc\theta & \cot\theta \end{bmatrix} \tag{8}$$

where Z_0 is the characteristic impedance of the line. A comparison of (7) and (8) suggests the equivalent circuit shown in Fig. 2. Note that the two unit elements have different electrical lengths. The $ABCD$ parameters may also be derived. These are indicated in Fig. 2.[1]

Next the short-circuited case will be considered. Shorting ports 2 and 4 in Fig. 1 imposes the boundary condition

$$V_2 = V_4 = 0.$$

The remaining two-port is described by the following equation:

$$\begin{bmatrix} I_1 \\ I_3 \end{bmatrix} = \begin{bmatrix} Y_{11} & Y_{13} \\ Y_{31} & Y_{33} \end{bmatrix} \begin{bmatrix} V_1 \\ V_3 \end{bmatrix} \tag{9}$$

where

[1] The Richards s-plane ($s=j\tan\theta$) notation (in which a capacitor represents an open-circuited stub of electrical length θ, an inductor represents a short-circuited stub, and a unit element, a length of transmission line), will be used in the figures.

$$\begin{bmatrix} Y_{11} & Y_{13} \\ Y_{31} & Y_{33} \end{bmatrix} = -j\frac{1}{2}\left[\begin{array}{c|c} Y_{0e}\cot\theta_e + Y_{0o}\cot\theta_o & -Y_{0e}\csc\theta_e + Y_{0o}\csc\theta_o \\ \hline -Y_{0e}\csc\theta_e + Y_{0o}\csc\theta_o & Y_{0e}\cot\theta_e + Y_{0o}\cot\theta_o \end{array}\right]$$
$$= -j\frac{Y_{0e}}{2}\left[\begin{array}{c|c} \cot\theta_e & -\csc\theta_e \\ \hline -\csc\theta_e & \cot\theta_e \end{array}\right] - j\frac{Y_{0o}}{2}\left[\begin{array}{c|c} \cot\theta_o & \csc\theta_o \\ \hline \csc\theta_o & \cot\theta_o \end{array}\right]. \tag{10}$$

Now the Y matrix for a simple unit element is

$$[Y] = -jY_0\begin{bmatrix} \cot\theta & -\csc\theta \\ -\csc\theta & \cot\theta \end{bmatrix} \tag{11}$$

where Y_0 is the characteristic admittance of the line. A comparison of (10) and (11) suggests the equivalent circuit shown in Fig. 3.

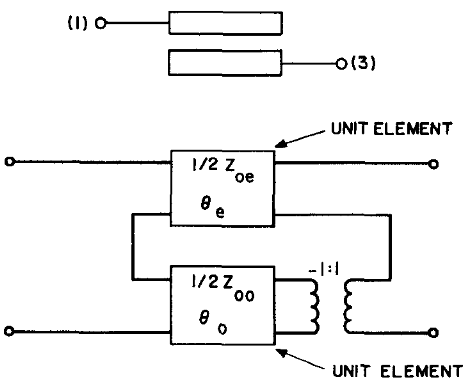

$$A = \frac{Z_{oe}\cot\theta_e + Z_{oo}\cot\theta_o}{Z_{oe}\csc\theta_e - Z_{oo}\csc\theta_o} = D;$$

$$B = \frac{j}{2}\,\frac{Z_{oe}^2 + Z_{oo}^2 - 2Z_{oe}Z_{oo}(\cot\theta_e\cot\theta_o + \csc\theta_e\csc\theta_o)}{Z_{oe}\csc\theta_e - Z_{oo}\csc\theta_o};$$

$$C = \frac{2j}{Z_{oe}\csc\theta_e - Z_{oo}\csc\theta_o}.$$

Fig. 2. Prototype open-circuited digital section.

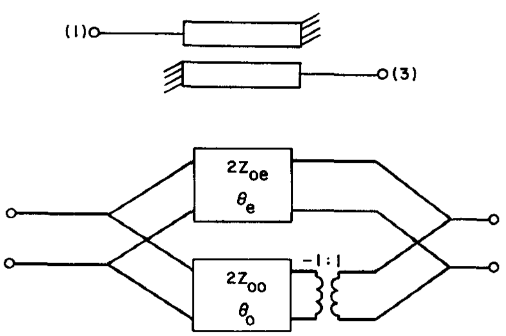

$$A = \frac{Y_{oe}\cot\theta_e + Y_{oo}\cot\theta_o}{Y_{oe}\csc\theta_e - Y_{oo}\csc\theta_o} = D;$$

$$B = \frac{2j}{Y_{oe}\csc\theta_e - Y_{oo}\csc\theta_o};$$

$$C = \frac{j}{2}\,\frac{Y_{oe}^2 + Y_{oo}^2 - 2Y_{oe}Y_{oo}(\cot\theta_e\cot\theta_o + \csc\theta_e\csc\theta_o)}{Y_{oe}\csc\theta_e - Y_{oo}\csc\theta_o}$$

Fig. 3. Prototype short-circuited digital section.

IV. Prototype Meander Line Sections

The basic circuit is constructed by tying together terminals 3 and 4 of the four-port in Fig. 1. This imposes the boundary conditions

$$V_3 = V_4; \qquad I_3 = -I_4.$$

The impedance matrix of the remaining two-port may be written as

$$Z = -j\frac{Z_{0e}}{2}\cot\theta_e\left[\begin{array}{c|c} 1 & 1 \\ \hline 1 & 1 \end{array}\right] + j\frac{Z_{0o}}{2}\tan\theta_o\left[\begin{array}{c|c} 1 & -1 \\ \hline -1 & 1 \end{array}\right]. \tag{12}$$

The equivalent circuit suggested by this impedance matrix consists of an open-circuited stub of characteristic impedance $Z_{0e}/2$ and electrical length θ_e connected in series with a short-circuited stub of impedance $Z_{0o}/2$ with length θ_0. The short circuited stub must be cascaded with a polarity reversing transformer. The equivalent circuit and the *ABCD* matrix of this two-port are given in Fig. 4.

In the homogeneous dielectric case, the above structure is the microwave type-C section (Zysman and Matsumoto [6]) which is an all-pass circuit. Here, however, the even and odd mode elements resonate at some frequencies creating a stop-band. The bandpass behavior of this section is confirmed by experimental results given later.

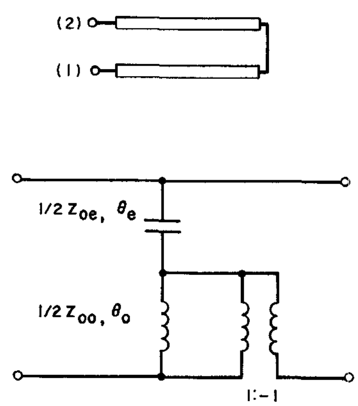

$$A = \frac{Z_{oe}\cot\theta_e - Z_{oo}\tan\theta_o}{Z_{oe}\cot\theta_e + Z_{oo}\tan\theta_o} = D;$$

$$B = \frac{2j\,Z_{oe}Z_{oo}\cot\theta_e\tan\theta_o}{Z_{oe}\cot\theta_e + Z_{oo}\tan\theta_o};$$

$$C = \frac{2j}{Z_{oe}\cot\theta_e + Z_{oo}\tan\theta_o}$$

Fig. 4. Meander line prototype section.

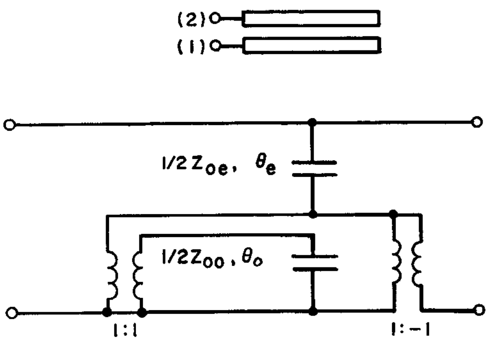

$$A = \frac{Z_{0e} \cot \theta_e + Z_{00} \cot \theta_0}{Z_{0e} \cot \theta_e - Z_{00} \cot \theta_0} = D;$$

$$B = -j \frac{2 Z_{0e} Z_{00} \cot \theta_e \cot \theta_0}{Z_{0e} \cot \theta_e - Z_{00} \cot \theta_0};$$

$$C = j \frac{2}{Z_{0e} \cot \theta_e - Z_{00} \cot \theta_0}.$$

Fig. 5. Comb line section.

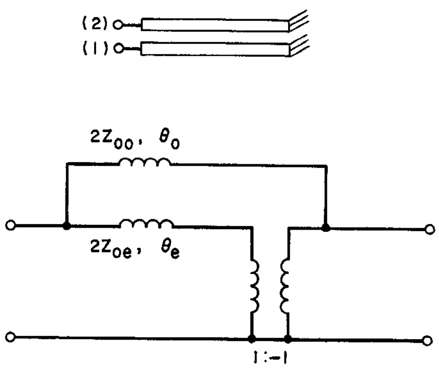

$$A = \frac{Y_{00} \cot \theta_0 + Y_{0e} \cot \theta_e}{Y_{00} \cot \theta_0 - Y_{0e} \cot \theta_e} = D;$$

$$B = j \frac{2}{Y_{00} \cot \theta_0 - Y_{0e} \cot \theta_e},$$

$$C = -j \frac{2 Y_{00} Y_{0e} \cot \theta_0 \cot \theta_e}{Y_{00} \cot \theta_0 - Y_{0e} \cot \theta_e}.$$

Fig. 6. Dual of Fig. 5.

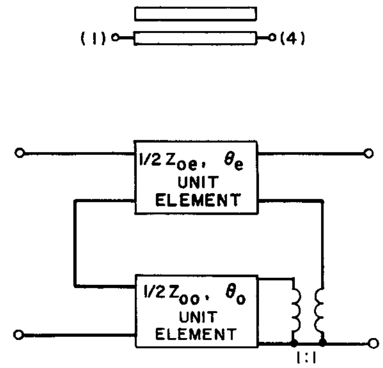

$$A = \frac{Z_{0e} \cot \theta_e + Z_{00} \cot \theta_0}{Z_{0e} \csc \theta_e + Z_{00} \csc \theta_0} = D;$$

$$B = j \frac{Z_{0e}^2 + Z_{00}^2 + 2 Z_{0e} Z_{00} (\csc \theta_e \csc \theta_0 - \cot \theta_e \cot \theta_0)}{2 (Z_{0e} \csc \theta_e + Z_{00} \csc \theta_0)};$$

$$C = j \frac{2}{Z_{0e} \csc \theta_e + Z_{00} \csc \theta_0}.$$

Fig. 7. Open-circuited symmetric structure.

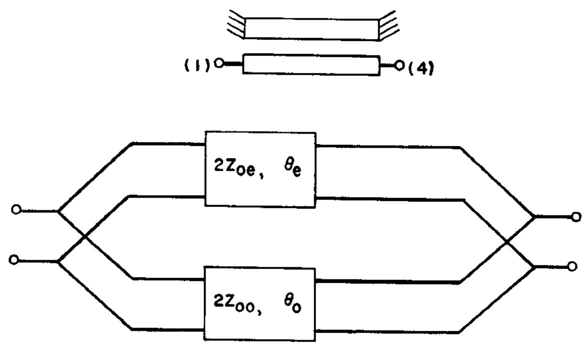

$$A = \frac{Y_{0e} \cot \theta_e + Y_{00} \cot \theta_0}{Y_{0e} \csc \theta_e + Y_{00} \csc \theta_0} = D;$$

$$B = j \frac{2}{Y_{0e} \csc \theta_e + Y_{00} \csc \theta_0};$$

$$C = j \frac{Y_{0e}^2 + Y_{00}^2 + 2 Y_{0e} Y_{00} (\csc \theta_e \csc \theta_0 - \cot \theta_e \cot \theta_0)}{2 \left[Y_{0e} \csc \theta_e + Y_{00} \csc \theta_0 \right]}.$$

Fig. 8. Short-circuited symmetric structure.

V. Comb Line Circuits

This circuit is constructed by open-circuiting terminals 3 and 4 in Fig. 1. This imposes the condition

$$I_3 = I_4 = 0.$$

The impedance matrix of this structure is

$$Z = -j \frac{Z_{0e}}{2} \cot \theta_e \left[\begin{array}{c|c} 1 & 1 \\ \hline 1 & 1 \end{array} \right] - j \frac{Z_{0o}}{2} \cot \theta_o \left[\begin{array}{c|c} 1 & -1 \\ \hline -1 & 1 \end{array} \right]. \tag{13}$$

The admittance matrix of the dual circuit in which

$$V_3 = V_4 = 0$$

is

$$Y = -j \frac{Y_{0e}}{2} \cot \theta_e \left[\begin{array}{c|c} 1 & 1 \\ \hline 1 & 1 \end{array} \right] - j \frac{Y_{0o}}{2} \cot \theta_o \left[\begin{array}{c|c} 1 & -1 \\ \hline -1 & 1 \end{array} \right]. \tag{14}$$

The equivalent circuits and the $ABCD$ parameters of the dual networks are shown in Figs. 5 and 6, respectively.

		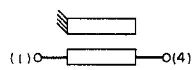	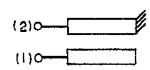
A	$\dfrac{2\cos\theta_0\cos\theta_e}{\cos\theta_0-\cos\theta_e}$	$\dfrac{2\cos\theta_0\cos\theta_e}{\cos\theta_0+\cos\theta_e}$	$\dfrac{Z_{0e}^2+Z_{00}^2-2Z_{0e}Z_{00}\csc\theta_e\csc\theta_0(\cos\theta_e\cos\theta_0+1)}{Z_{0e}^2-Z_{00}^2}$
B	$j\dfrac{Z_{00}\sin\theta_0\cos\theta_e+Z_{0e}\cos\theta_0\sin\theta_e}{\cos\theta_0-\cos\theta_e}$	$j\dfrac{Z_{00}\sin\theta_0\cos\theta_e+Z_{0e}\cos\theta_0\sin\theta_e}{\cos\theta_0+\cos\theta_e}$	$-j\dfrac{2Z_{0e}Z_{00}(Z_{00}\cot\theta_e+Z_{0e}\cot\theta_0)}{Z_{0e}^2-Z_{00}^2}$
C	$j\dfrac{Y_{00}\sin\theta_0\cos\theta_e+Y_{0e}\cos\theta_0\sin\theta_e}{\cos\theta_0-\cos\theta_e}$	$j\dfrac{Y_{00}\sin\theta_0\cos\theta_e+Y_{0e}\cos\theta_0\sin\theta_e}{\cos\theta_0+\cos\theta_e}$	$-j\dfrac{2(Z_{0e}\cot\theta_e+Z_{00}\cot\theta_0)}{Z_{0e}^2-Z_{00}^2}$
D	$\dfrac{2(\cos\theta_0\cos\theta_e-1)-\sin\theta_0\sin\theta_e(Y_{00}Z_{0e}+Z_{00}Y_{0e})}{2(\cos\theta_0-\cos\theta_e)}$	$\dfrac{2(\cos\theta_0\cos\theta_e+1)-\sin\theta_0\sin\theta_e(Y_{00}Z_{0e}+Z_{00}Y_{0e})}{2(\cos\theta_0+\cos\theta_e)}$	$\dfrac{Z_{0e}^2+Z_{00}^2-2Z_{0e}Z_{00}\csc\theta_e\csc\theta_0(\cos\theta_e\cos\theta_0-1)}{Z_{0e}^2-Z_{00}^2}$

Fig. 9. Unsymmetric networks.

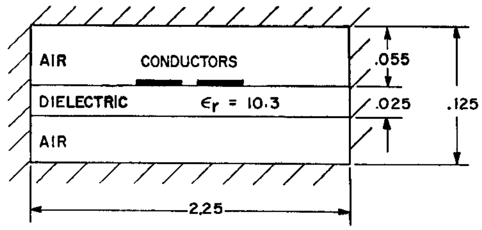

Fig. 10. Cross-sectional schematic of box.

VI. Other Structures

The equivalent circuits of the remaining two symmetric networks are readily derived. For the circuit shown in Fig. 7,

$$I_2 = I_3 = 0$$

and

$$Z = -j\frac{Z_{0e}}{2}\left[\begin{array}{c|c} \cot\theta_e & \csc\theta_e \\ \hline \csc\theta_e & \cot\theta_e \end{array}\right] - j\frac{Z_{0o}}{2}\left[\begin{array}{c|c} \cot\theta_o & \csc\theta_o \\ \hline \csc\theta_o & \cot\theta_o \end{array}\right]. \tag{15}$$

The equivalent circuit and the $ABCD$ parameters are given in Fig. 7. The dual network and its characterization is shown in Fig. 8.

The unsymmetric networks do not readily lend themselves to equivalent circuit representations. However, their $ABCD$ matrices may be derived. These are indicated in Fig. 9.

It is of interest to note that in the first unsymmetric digital structure of Fig. 9 the mutual impedance between ports 1 and 3 is

$$z_{13} = j\frac{Z_{0o}Z_{0e}\csc\theta_o\csc\theta_e(\cos\theta_o - \cos\theta_e)}{Z_{0e}\cot\theta_e + Z_{0o}\cot\theta_o}. \tag{16}$$

This is in contrast to the homogeneous dielectric case in which this mutual impedance is zero.

Through the use of these equivalent circuits or the $ABCD$ parameters it is possible to obtain simple theoretical predictions, given the even and odd mode characteristics of two equal coupled lines.

VII. Experimental Results

Transmission loss measurements have been made on several of the above types of networks. The circuits were deposited on a structure which was suspended in a box as shown in Fig. 10 (all dimensions in inches). The interdigital circuits were considered first. Ten circuits, each composed of two open-circuited lines of width 0.120 inch and gap spacings ranging from 0.0031 to 0.0403 inch were investigated.

Had the lines been constructed in a homogeneous medium the transmission response would have had a bandpass characteristic with the center of the passband located at that frequency where the lines were a quarter-wavelength long electrically. The experimental results for the lines in the homogeneous media are found to be quite different from this. The primary characteristic is a peak of high transmission loss (or bandstop region) at a frequency well above either f_{0e} or f_{0o}, and this type of response is indeed predicted by the equivalent circuit of Fig. 2.

The theoretical characteristics of the test circuits have been calculated through use of this equivalent circuit. The center frequency of the bandstop region has been determined and in order to also determine how closely the equivalent circuit will predict the overall response of the coupled lines, the frequencies (on either side of the center frequency) at which the loss is down to 10 dB have also been calculated and measured. These results are tabulated and shown in Table I. It can be seen that the center frequency predictions are all within 1 percent of the corresponding measured results, and the 10 dB frequencies are all within 3 percent. A typical response plot is shown in Fig. 11.

Similar calculations and measurements have been made

TABLE I

EXPERIMENTAL AND THEORETICAL RESULTS

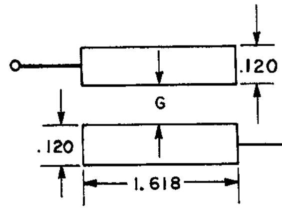

G IN INCHES	CENTER f(GHz) THEORETICAL	CENTER f(GHz) EXPERIMENTAL	% DIFFERENCE	LOWER 10 dB f(GHz) THEORETICAL	LOWER 10 dB f(GHz) EXPERIMENTAL	% DIFFERENCE	UPPER 10 dB f(GHz) THEORETICAL	UPPER 10 dB f(GHz) EXPERIMENTAL	% DIFFERENCE
.0031	1.661	1.665	-0.24	1.555	1.597	-2.66	1.749	1.754	-0.29
.0053	1.649	1.659	-0.60	1.517	1.529	-0.79	1.750	1.763	-0.74
.0072	1.665	1.666	-0.06	1.519	1.527	-0.53	1.776	1.781	-0.28
.0102	1.674	1.672	0.12	1.509	1.501	0.53	1.800	1.807	-0.39
.0156	1.682	1.685	-0.18	1.484	1.482	0.13	1.832	1.825	0.38
.0202	1.690	1.691	-0.06	1.464	1.463	0.07	1.860	1.867	-0.38
.0253	1.692	1.678	0.83	1.434	1.428	0.42	1.882	1.876	0.32
.030	1.697	1.683	0.83	1.408	1.412	-0.28	1.906	1.915	-0.47
.0356	1.714	1.710	0.23	1.384	1.363	1.53	1.950	1.972	-1.12
.0403	1.709	1.710	-0.06	1.344	1.340	0.30	1.964	1.987	-1.16

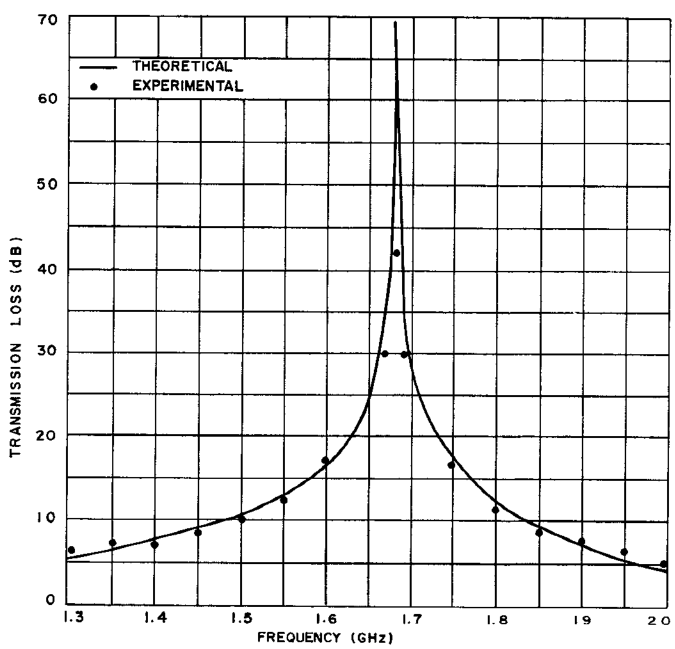

Fig. 11. Transmission loss for typical interdigital circuit ($G=0.0156$).

for the circuits shown in Figs. 4 and 7. These results are shown in Tables II and III. It can be seen that the center frequency predictions are all within 2.1 percent of the corresponding measured results, and the skirt frequencies are all within 3 percent.

VIII. CONCLUSIONS

The effects of electromagnetic coupling in parallel-conductor inhomogeneous transmission lines were considered here. It was shown that the characteristics of various coupled-line circuits embedded in an inhomogeneous dielectric (such as the suspended substrate) differ markedly from those in a homogeneous environment. The theory has been tested experimentally and the agreement is very good.

The *ABCD* parameters of all circuits, investigated by Jones and Bolljahn [1], were derived for an inhomogeneous dielectric medium. From these, response of various composite circuit configurations may be calculated. The even and

TABLE II

EXPERIMENTAL AND THEORETICAL RESULTS FOR MEANDER LINE CIRCUITS

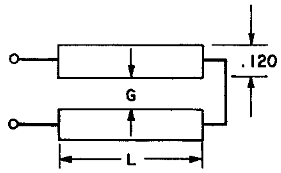

L IN INCHES	G IN INCHES	CENTER f (GHz) THEO-RETICAL	CENTER f (GHz) EXPERI-MENTAL	% DIF-FERENCE	LOWER f (GHz) THEO-RETICAL	LOWER f (GHz) EXPERI-MENTAL	% DIF-FERENCE	UPPER f (GHz) THEO-RETICAL	UPPER f (GHz) EXPERI-MENTAL	% DIF-FERENCE
1 5840	.0033	2 873	2.828	1.59	2.748	2.712 (10dB)	1.33	2.991 (10dB)	2.954	1 25
1 5936	0055	2.938	2 979	-1.37	2.798	2.838 (10dB)	-1.41	3 081 (10dB)	3.175	-1.39
1 5975	.0085	3.027	3 010	0.57	2.941	2.922 (15dB)	0.65	3.118	3.117 (15dB)	0.03
1 6030	.0125	3.133	3.112	0.68	3.076	3.044 (20dB)	1.05	3.194	3.171 (20dB)	0.79

TABLE III

EXPERIMENTAL AND THEORETICAL RESULTS FOR CIRCUITS OF FIG. 7

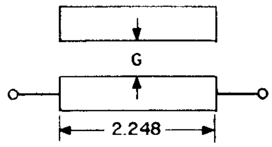

G IN INCHES	CENTER f (GHz) THEO-RETICAL	CENTER f (GHz) EXPERI-MENTAL	% DIF-FERENCE	LOWER f (GHz) THEO-RETICAL	LOWER f (GHz) EXPERI-MENTAL	% DIF-FERENCE	UPPER f (GHz) THEO-RETICAL	UPPER f (GHz) EXPERI-MENTAL	% DIF-FERENCE
.0034	1.457	1.435	1.53	1.420	1.397 (6 dB)	1.65	1.504	1.472 (6 dB)	2.17
.0058	1.498	1.486	0.81	1.476	1.464 (10dB)	1.82	1.524	1.508 (10dB)	1 06
.0086	1535	1 524	0.72	1.513	1.504 (10dB)	0.60	1.559	1.545 (10dB)	0.91
0123	1.573	1.555	1.16	1.552	1.535 (10dB)	1.11	1.596	1.576 (10dB)	1 2 7
0203	1.637	1.615	1.36	1.618	1.598 (10dB)	1.25	1657	1.633 (10 dB)	1 4 7
0406	1 738	1.702	2.10	1.715	1.679 (6 dB)	2.14	1.763	1.725 (6 dB)	2 20

odd mode propagation constants and characteristic impedances must, of course, be obtained numerically first. It is hoped that the equivalent circuits derived here will prove a useful tool in filter synthesis.

ACKNOWLEDGMENT

The authors would like to express their gratitude to W. W. Mumford for his generous advice and encouragement and to J. I. Smith for his great help in providing the theoretical values of the even and odd mode capacitances in the suspended substrate lines. Thanks are also due to J. M. DelColle for his assistance in obtaining the experimental results.

REFERENCES

[1] E. M. T. Jones and J. T. Bolljahn, "Coupled-strip-transmission line filters and directional couplers," *IRE Trans. Microwave Theory and Techniques*, vol. MTT-4, pp. 75–81, April 1956.
[2] S. O. Rice, "Steady-state solutions of transmission line equations," *Bell Sys. Tech. J.*, vol. 20, pp. 131–178, April 1941.
[3] E. G. Vlostovskiy, "Theory of coupled transmission lines," *Telecommun. and Radio Engrg.*, vol. 21, pp. 87–93, April 1967.
[4] M. Murray, private communication, 1965.
[5] J. I. Smith, "The even and odd mode capacitance parameters for coupled lines in suspended substrate," presented at the 1969 G-MTT Internatl. Microwave Symp., Dallas, Tex., paper TPM-II-8.
[6] G. I. Zysman and A. Matsumoto, "Properties of microwave C-sections," *IEEE Trans. Circuit Theory*, vol. CT-12, pp. 74–82, March 1965.